

Progress in Relating Rare Earth Ion 4f and 5d Energy Levels to Host Bands in Optical Materials for Hole Burning, Quantum Information, and Phosphors

C. W. THIEL, Y. SUN, and R. L. CONE

Department of Physics, Montana State University, Bozeman, MT 59717

Abstract. Rare earth ions play an important role in modern technology as optically active elements in solid-state luminescent materials. In many of these materials, interactions between the electronic band states of the host crystal and the rare earth ion's localized $4f^N$ and $4f^{N-1}5d$ states influence the material's optical properties. The importance of these interactions is discussed for material applications in photon-gated hole burning, quantum information, and phosphors. Material dependent trends in the relative binding energies of the $4f^N$ states and the host bands have been observed and are summarized. An empirical model for the ion dependence of the 4f electron binding energies is formulated in terms of atomic number and compared to previous models. These models are extended to describe the $4f^{N-1}5d$ states with one additional parameter. Improved estimates for the free-ion ionization potentials used in the model are also presented and discussed.

Version Date: April 19, 2002

1. Introduction

Rare earth ions, also referred to as lanthanides, play an important role in modern technology as the active constituents of many optical materials. There are a vast number of applications for these rare-earth-activated materials and much of today's cutting-edge optical technology and emerging innovations are enabled by their unique properties. Specific applications may employ the rare earths' atomic-like $4f^N$ to $4f^N$ optical transitions when long lifetimes, sharp absorption lines, and excellent coherence properties are required, while others may employ the $4f^N$ to $4f^{N-1}5d$ transitions when large oscillator strengths, broad absorption bands, and shorter lifetimes are desirable.

In many applications, interactions between the rare earth ion and the electronic states of the host material can enhance or inhibit performance and provide mechanisms for manipulating the material's optical properties. Although the general properties of the rare earths' electronic states and transitions are well understood and their theoretical description is well established [1], much less is known regarding the relationships between the energy levels of the rare earth ions and the electronic band states of the crystal lattice. Developing a complete picture of the electronic structure of rare-earth-activated insulators that incorporates these relationships is essential for understanding interactions between these states and how they influence basic material properties.

In recent years, there have been a steadily increasing number of studies to extend our understanding of the relationships between the rare earth and host electronic states and how they affect the optical properties of specific interest for technological applications. The relative energies of these states have been explored using a wide variety of techniques including excited-state absorption [2, 3], photoluminescence excitation [4], photoconductivity [5-7], and electron photoemission [8-10]. In addition to the need for determining the energies of the rare earth's electronic states relative to the host states, it has been shown that dynamic interactions between these states is important for understanding the luminescence of many materials [4, 11].

To improve our fundamental physical understanding of these phenomena as well as to provide new information of practical significance for technological applications, we have recently adopted a systematic approach to the study of the relative energies and the interaction dynamics of the rare earth energy levels and the host bands in optical materials [10, 12, 13]. In this paper, we outline our progress in understanding these phenomena and how they influence important applications.

2. Applications

Interactions between host band states and rare earth energy levels have a broad impact on technologically significant applications of rare-earth-activated optical materials. Lasers, plasma displays, fluorescent lamps, solid-state lighting, medical imaging, and optical computing technologies are just a few of the applications that would benefit from a practical understanding of these interactions. The influence of these interactions on applications clearly indicates that understanding and identifying material trends would dramatically accelerate the development of performance-optimized materials.

Rare earth phosphors for lamps and displays are a prominent example of a technology where interactions between the rare earth energy levels responsible for the luminescence and the host band states can strongly influence performance. In the search

for new materials for solid-state lighting and mercury-free fluorescent lamps, the emission of potential phosphor materials is often limited or completely quenched due to ionization of the excited rare earth ion [11]; in contrast, charge transfer absorption provides a mechanism for efficiently pumping phosphors such as $\text{Eu}:\text{Y}_2\text{O}_3$ while charge transfer luminescence may provide a new mechanism for phosphor materials [14]. The stark contrast between the complete lack of radiative emission in proposed $\text{Ce}:\text{Y}_2\text{O}_3$ phosphors and the efficient $\text{Eu}:\text{Y}_2\text{O}_3$ commercial red phosphors used for large-area plasma display screens and fluorescent lamps has also inspired photoconductivity studies of Ce^{3+} in Y_2O_3 and related hosts. These studies have shown that the failure of these materials as phosphors results from non-radiative decay through relaxation pathways involving the host conduction band [7, 11]. It has also been shown that lattice relaxation effects associated with ionization of the rare earth ion are extremely important for understanding many of the luminescence properties of these materials [4, 15]. All of these results suggest that developing a unified picture for the electronic structure of rare-earth-activated materials that includes the electronic states of both the active ion and the host crystal would provide valuable insight into the luminescence of current phosphors and help guide the development of new phosphors to enable the next generation of lighting and display technology.

An example of a technology that may specifically exploit these interactions is photon-gated spectral hole burning. In spectral hole burning, a narrow-band laser is used to reduce the absorption at specific frequencies by selectively exciting the subset of ions in the material that absorb at the laser frequency. The resulting increase in transmission, or “hole” in the absorption, persists until the excited ions relax back to their ground state. If the ions decay from the excited state to a metastable “bottleneck” state rather than directly to the ground state, the spectral hole may persist for the lifetime of the bottleneck state. This basic process may be used in a wide variety of technologies ranging from laser frequency stabilization [16, 17] to high-speed optical computation and memories using spatial-spectral holography [18, 19].

In the basic hole burning process, additional hole burning that occurs when probing the material with “readout” photons may partially erase the information stored in the absorption profile. Photon-gated spectral hole burning is a two-photon process in which the first photon provides the spectral selectivity by exciting the ion, and a second “gating” photon is required to enable the hole burning mechanism. This gated hole burning process provides a method for non-destructive readout of the information stored in the absorption profile since hole burning only occurs when the gating photons are present. One mechanism that is well-suited to photon-gating is two-step photoionization [20, 21]. The steps involved in this mechanism are illustrated in Fig. 1. In the first step, a laser selectively excites a $4f^N$ to $4f^N$ transition of ions at frequencies where spectral holes are to be burned. Next, the gating photons selectively excite the ions that are in their upper $4f^N$ state to a $4f^{N-1}5d$ state. Because of the large oscillator strength and broad absorption of the $4f^N$ to $4f^{N-1}5d$ transition, either a second laser or even possibly a filtered broadband lamp could be used as the source of gating photons to excite the ions into the $4f^{N-1}5d$ state. If the $4f^{N-1}5d$ state is within the conduction band of the host, the 5d electron may relax into the conduction band and diffuse away from the rare earth ion to become trapped at an electron acceptor site in the lattice (lattice defects or doped acceptor

impurities). Since the valence of the excited rare earth ion has changed, it is permanently removed from the absorption, producing a persistent spectral hole.

Photon-gated spectral hole burning has important applications including laser frequency stabilization, optical coherent transient data processing, and optical memories. In the laser frequency stabilization applications, a narrow spectral hole burned at the desired laser frequency may be used as a reference to stabilize the laser [16, 17]. These stable lasers have many applications in both fundamental research, where they enable measurements over long time scales with Hertz-level resolution, and technological applications such as measuring precise distances through interferometry. Photon-gated hole burning is of particular interest for laser stabilization since it prevents the laser from modifying the spectral hole during the locking process. In optical data processing and memory applications, photon-gated hole burning would provide a mechanism for “programming” the material by modifying the absorption spectrum while providing for non-destructive readout by avoiding hole burning from probe photons.

Photon-gated hole burning may also prove useful in proposed architectures for quantum information applications that employ entangled states of rare earth ions in a crystal. Some of these techniques involve generating spectral features that correspond to groups of strongly coupled ions in the lattice [22, 23]. This is done by using hole burning to selectively remove ions from the absorption spectrum until only the coupled ions remain. In these methods, photon-gating potentially could be used to permanently remove the undesired ions from the absorption spectrum when preparing the material.

The first step in developing practical photon-gated photoionization hole burning materials for each of these applications is to determine the energies of the $4f^{N-1}5d$ states relative to the host conduction band as well as the energies of the $4f^N$ ground states relative to the host valence band. For the ionization hole burning process to produce stable, long-lived spectral holes, it is expected that the $4f^N$ ground state must have an energy higher than the valence band states. The reason is that, if there are occupied valence states at higher energy than the $4f^N$ ground state, an electron from the ligand ions, whose valence states primarily contribute to the valence band, can relax into the “hole” on the ionized rare earth, returning the rare earth to its original valence and filling the spectral hole. In addition, it is important to know the energy of the $4f^{N-1}5d$ states relative to the conduction band to determine which levels are degenerate with conduction band states and what corresponding gating wavelength is required to produce ionization. This approach has recently been applied to rare-earth-doped $YAlO_3$, where the energies of the $4f^N$ and $4f^{N-1}5d$ states relative to the host band states were determined and discussed within the context of photon-gated photoionization hole burning [24]. This work indicates that by extending these methods to additional materials, potential photoionization hole burning materials may be identified and analyzed to determine whether they are suitable candidates.

3. Recent Progress

To better understand the relationships between the rare earth $4f^N$ and $4f^{N-1}5d$ states and the host band states as well as to provide practical information for the development of new materials, we have employed conventional electron photoemission and resonant photoemission to measure the relative energies of the $4f^N$ and host valence band states in optical materials [10, 12]. Photoemission allows the energies of occupied electronic

states to be independently measured relative to an absolute energy reference and complements optical methods, which measure energy differences between electronic states in the material. By determining the energies of electronic states using photoemission, features that appear, or do not appear, in the optical spectra may be unambiguously interpreted in terms of energy differences and transition probabilities—two properties that are difficult to deconvolve from the optical spectra alone. Furthermore, resonant photoemission spectroscopy allows the rare earth 4f electron photoemission to be clearly identified and separated from the host spectrum by using synchrotron radiation to probe resonances in the rare earth photoemission cross-section. Because the precise energy of the photoemission resonance is an atomic property that is unique to each ion and valence state, resonant photoemission may be used to separate and identify each rare earth ion and rare earth valence state present within a material. By observing the systematic changes in the relative energies for different states, ions, and host materials, insight is gained into electron transfer, luminescence quenching, and ion valence stability.

It has been shown that a simple two-parameter empirical model accurately describes the binding energies of the $4f^N$ states for all rare earth ions in materials ranging from ionic insulators to covalent metals [10, 12]. Since the model only requires two parameters to describe the effect of the host material, measurements on just two ions in a material can be used to predict the energies of all other rare earth ions in that material. It has also been suggested that, in some materials, measurements on a single ion and the host material itself may be sufficient to determine the energies of the remaining ions [10]. This empirical approach provides an important tool for practical material development and may provide fundamental information about the material when viewed within the theoretical frameworks that describe the effect of the material on the rare earth binding energies.

In the following sections, we discuss our recent progress in understanding, explaining, and predicting the energies of the localized electronic states of the rare earth ions relative to the host band states. In Section 3.1, refinements of the empirical model are presented that both improve its accuracy and extend its applicability. In Section 3.2, we discuss an extension of the empirical model that includes the important $4f^{N-1}5d$ states of the rare earth ions. Finally, Section 3.3 provides a short summary of several material dependent trends in the rare earth binding energies that have been observed for the materials so far studied.

3.1. *Refinements of the Empirical Model*

The practical utility of an empirical model has stimulated our recent work in applying a simple two-parameter model to the description, analysis, and extrapolation of binding energies in optical materials [10, 12]. The particular form of this empirical model was originally motivated by the extensive work that has been done over the last century using an electrostatic point-charge model for the effect of the lattice on the electron binding energies. In this picture, the binding energies of an ion's electrons are viewed as being the free-ion values shifted through interactions with the lattice. These effects include the Madelung potential of the lattice site, the polarizability of the material, inter-atomic repulsive energies, and smaller effects such as Van der Waal's energies [25-27]. A further complication in optical materials is that the active ion is commonly an

impurity rather than a normal lattice constituent; thus, the local distortion of the lattice induced by the presence of the impurity can cause a significant change in the site's Madelung potential that results in a corresponding shift in the binding energies [5]. This picture leads to an empirical model of the form $E_{4f} = I - E_L + \alpha_R(R - R_0)$, where E_{4f} is the 4f electron binding energy relative to a free electron in vacuum, I is the free-ion ionization potential, E_L is a binding energy shift experienced by all rare earth ions in a material, and $\alpha_R(R - R_0)$ represents an ion dependent shift in binding energy when the substituted rare earth's ionic radius R deviates from the normal host ion's radius R_0 . These definitions are chosen so that E_L represents a parameter that may be directly measured from the host lattice itself, since it is just the binding energy shift experienced by the normal lattice constituent [10]. If we wish to reference the binding energies relative to another energy such as the valence band maximum, an additional term may be explicitly included in the model to subtract off the reference energy, or the reference energy may be included implicitly in the definition of E_L . For ionic materials where the electrostatic point-charge model is most appropriate, the parameters in this model may be directly estimated using the theoretical model of Pedrini et. al. [5, 6] if sufficient information is available for both the lattice and the effect of the impurity-induced distortion. In covalent materials such as the metals, chemical considerations have also led to a model for the binding energies in which the free-ion values are shifted because of the redistribution of charge and electrostatic shielding that occurs in the solid [28, 29]. In this picture, it is the variation in the effective nuclear charge experienced by the valence electrons that produces an ion-dependent binding energy shift in the material. Within this framework, the ionic radius that enters into the empirical model may be viewed as an estimate for the effective nuclear charge experienced by the valence electrons of the rare earth ion; hence, the model is also successful for describing covalent materials.

Although the empirical model can be shown to be an approximate expression for the binding energy in ionic and covalent materials, the extremely simple form of the model lends itself to an even more basic perspective. Specifically, we may view the empirical model as just the first two terms of a Taylor's series expansion for *any* effect of the lattice on the binding energy, where the expansion variable is the ionic radius of the ion—a physical parameter that directly influences the ion's environment. This simple interpretation may provide some insight into why the model applies to such a wide range of materials and cautions against too stringent an interpretation of the empirical parameters within a specific theoretical framework.

Another implication of this view is that perhaps another variable may be chosen when performing the expansion. To explore this possibility, we may consider a model of the form $E_{4f} = I - E_L + \alpha_A(A - A_0)$, where E_{4f} , I , and E_L have the same meaning as previously, and $\alpha_A(A - A_0)$ represents an ion dependent shift in binding energy that simply depends on the ion's atomic number A . In this model, a value of $A_0 = 67$ is chosen so that E_L has approximately the same value and interpretation as in previous work that used trivalent yttrium as the ionic radius reference [10, 12]. The choice of atomic number as the variable to describe the ion-dependence is motivated by the simplicity and generality of the expression as well as indications that it may represent an appropriate description for more covalent materials. Because the ionic radius is nearly linear as a function of atomic number, this form of the model gives nearly identical predictions for the 4f electron binding energies, with deviations smaller than the experimental accuracies currently

achievable by any experimental method. As an example, in Fig. 2 the two models are compared to the measured 4f electron binding energies in the elemental rare earth metals from Lang et. al. [30]. The rare earth metals represent the most accurately known set of 4f binding energies available since the experimental features are much sharper in the metals than in other materials. Furthermore, the magnitude of the ion dependent term is nearly 2.5 times larger in the metals than in the other materials that have been studied; therefore, the metals represent an extreme case in which the differences between the two forms of the model are maximized. In Fig. 2, the circles are experimental binding energies (relative to the Fermi energy), the solid line is the fit of the model using the ionic radius, and the dotted line is the fit of the model using the atomic number. Comparison of the two fits indicates that both expressions describe the binding energies equally well to within the experimental accuracy, with an approximate relationship between the parameters of $\alpha_A \approx -0.013\alpha_R$ —a correspondence that also approximately holds for the other materials that we have studied. The agreement between the two forms of the model is expected to be even closer for the majority of optical materials, implying that either form may be used interchangeably as an empirical expression for the 4f electron binding energies.

The two forms of the empirical model each present different advantages and disadvantages. The use of ionic radius in the model has a clearer physical interpretation and may be directly related to theoretical models in ionic materials [5]. However, ambiguity may arise because the ionic radius depends on both the environment of the ion and the degree of covalency in the bonding. Using the atomic number in the model provides a simple approach in which there is no ambiguity. However, this approach is more difficult to directly relate to theoretical models. Another advantage of the atomic number approach is that it allows a straightforward comparison of the parameters obtained from different materials regardless of the nature of the environment or the bonding. This might permit material trends to be more easily identified and analyzed. Thus, the choice of a particular form of the empirical model primarily depends on the intended application.

In both the empirical and theoretical models for the rare earth electron binding energies, the free-ion ionization potentials play an important role. Unfortunately, many of the existing ionization potential values have relatively large uncertainties that directly affect the accuracy of models that incorporate them. It has been suggested [10] that improved estimates for the free-ion ionization potentials might be obtained by comparing experimental electron energies in solids to the empirical model for the binding energies. With the goal of improving the accuracy of the empirical model, we have analyzed the systematic deviations between experimental energies and the empirical model to obtain a set of “effective” free-ion ionization potentials as listed in Table 1. These values were obtained by analyzing the available experimental energies of rare earth ions in the garnets [10, 12], the rare earth metals [30], the rare earth fluorides [31], La_2S_3 [31], and YAlO_3 [24, 31]. Deviations between the measured binding energies and the fit of the model were simply viewed as arising from a combination of the experimental error of each measurement and the error in the model due to uncertainties in the free-ion ionization potentials. Thus, by choosing ionization potentials that give perfect agreement between the model and the experimental data points, a set of new estimates for the free-ion ionization potentials are obtained from each material that have an uncertainty

approximately equal to the experimental error. The estimated ionization potentials from each material were then averaged together with the experimental values for the free ions [32] to obtain the best final estimates, where each experimental value was weighted by its uncertainty in the averaging process using the standard statistical method. The effective ionization potentials obtained from this procedure are presented in Table 1, along with the corresponding uncertainty in each value.

To demonstrate the impact of these effective ionization potential parameters on the $4f^N$ binding energy model, the fit of the empirical model using these new values is shown for yttrium aluminum garnet in Fig. 3. The circles represent experimental binding energies [2, 6, 10], the dotted line is the fit of the model using the free-ion ionization potentials [32], and the solid line is the fit using the effective ionization potentials from Table 1. Only the values for europium and gadolinium are significantly different (the free-ion values for those two ions had large uncertainties), with the remaining ions only experiencing modest shifts. However, the estimated uncertainties were improved for nearly all of the ions—an important result for the empirical model since the errors must be incorporated as weighting factors in the fitting process. By comparing the two curves to the experimental data, we can clearly see that the large deviation previously observed for the gadolinium binding energy was primarily due to the error in the free-ion ionization potential used in the model. For rare earths whose measured free-ion ionization potentials are relatively uncertain, such as gadolinium, these effective values may represent improved estimates for the free-ion values. However, care must be taken when interpreting the precise meaning of these effective ionization potentials since, in addition to representing corrections to values for the free ions, they may also include corrections for any systematic deviations inherent in the empirical model itself. In any case, these values represent a significant improvement in the accuracy of the empirical model, with future work on additional materials promising to provide even greater improvements.

3.2. Extending the Picture to Include $4f^{N-1}5d$ States

The $4f^{N-1}5d$ states of the rare earth ions are important for many applications, some of which were outlined in Section 2. To obtain fundamental information about each material and evaluate its suitability for particular applications, we wish to determine the energies of the $4f^{N-1}5d$ states relative to the host band states. These relative energies may be determined by combining the measured or predicted binding energies of the $4f^N$ states relative to the host bands and the measured energy differences between the $4f^N$ and $4f^{N-1}5d$ states [24]. The barycenters of the $4f^N$ to $4f^{N-1}5d$ transition energies, which exhibit large variations from material to material, may be determined from the absorption spectra of each rare earth ion in the host material. As an example of this procedure, the binding energies of the lowest $4f^{N-1}5d$ states in yttrium aluminum garnet were determined, as shown in Fig. 4 by the triangles. The circles represent the average of the measured $4f^N$ binding energies from Refs. [2, 6, 10], and the solid line is the fit of the empirical model using the effective ionization potentials from Table 1. These $4f^N$ energies were combined with the $4f^N$ to $4f^{N-1}5d$ transition energies from Refs. [33, 34] to obtain the $4f^{N-1}5d$ binding energies. These binding energies may be interpreted as the energy required to remove the 5d electron from the $4f^{N-1}5d$ configuration, leaving the tetravalent ion with a $4f^{N-1}$ configuration in the lowest energy state.

By incorporating existing empirical models for the $4f^N$ to $4f^{N-1}5d$ transition energies into the $4f^N$ binding energy model, we may obtain an empirical model that describes both the $4f^N$ and $4f^{N-1}5d$ binding energies of all rare earth ions in a host material. Several models for the $4f^N$ to $4f^{N-1}5d$ transition energies have been applied to the study of optical materials over the last four decades [35-38]. Recently, Dorenbos [34, 39] has compiled experimental measurements for hundreds of materials, and by comparing these experimental values with the theoretical models for the transition energies, has developed a simple empirical model in which only a single material dependent energy shift is required to determine the lowest $4f^N$ to $4f^{N-1}5d$ transition for all rare earth ions. Thus, by combining the empirical model for the $4f^N$ to $4f^{N-1}5d$ transition energies with the model for the $4f^N$ binding energies, a simple model is obtained that describes both the $4f^N$ and $4f^{N-1}5d$ binding energies in a material using only three empirical parameters. This is shown in Fig. 4 for yttrium aluminum garnet by the dotted lines. For the second half-series, the lower and upper dotted lines represent the barycenters of the lowest energy high-spin and low-spin $4f^{N-1}5d$ levels, respectively.

It is important to note that, in contrast to the $4f^N$ energies, the $4f^{N-1}5d$ binding energies have similar values for all of the rare earth ions. This similarity is expected since the large variation in $4f^N$ to $4f^{N-1}5d$ transition energy arises primarily from the strong electron correlation in the $4f^N$ configuration, with the energy of the 5d valence state only weakly influenced by the nature of the tetravalent $4f^{N-1}$ core. However, we do observe variation of as much as 1 eV across the rare earth series, indicating that the 5d levels cannot be taken to have exactly the same absolute binding energies.

The success of this model implies that, once the $4f^N$ energies are known, a single binding energy measurement of a rare earth ion's lowest $4f^{N-1}5d$ state in a material is sufficient to predict the energy of the lowest $4f^{N-1}5d$ states for all the remaining ions. This picture provides important insight into the behavior of the $4f^{N-1}5d$ luminescence in optical materials and is a powerful tool for the development of new optical materials, with particular significance in the search for photon-gated spectral hole burning materials.

3.3. Observation of Material Trends

One of the primary goals of our work is to search for material dependent trends in the relative energies of the rare earth $4f^N$ states and the host band states. Although this work is in its early stages, several important trends have been identified in the materials so far studied.

Recently, a series of rare earth garnets have been studied for concentrations ranging from a few percent to the stoichiometric compounds. In these materials, it was found that the host valence band and the 4f electron binding energies were not affected by the rare earth ion concentration, maintaining the same values across the entire range of concentrations to within the experimental accuracy [10]. In addition, measurements on the aluminum, gallium, and iron garnets indicated that the 4f electron energies maintained the same absolute binding energies, while the valence band was shifted to reduced binding energies going from aluminum to gallium to iron [12]. Thus, in these materials, the systematic shifts between the $4f^N$ energies and the host bands arise entirely from shifts of the host bands. We might also expect similar composition dependent trends to be observed in related ternary compounds such as $YAlO_3$.

When examining a wider range of materials, simple trends may be observed in the empirical parameters that describe the $4f^N$ binding energies. For example, when comparing chemically similar materials such as $Y_3Al_5O_{12}$ and $YAlO_3$, we have observed that the variations in the binding energies of the $4f^N$ electron energies between the materials arise almost entirely from the ion-dependent term in the model (α_R or α_A), with the same binding energy shift parameter (E_L) observed. However, when comparing results from chemically different materials, such as the oxides and fluorides, both parameters in the model can vary significantly. By identifying simple trends such as these, insight is gained into the behavior of the $4f^N$ energies in different materials. This insight can be extremely important for understanding the optical properties of rare earth materials and for guiding the development of materials for applications such as hole burning, quantum information, and phosphors.

Acknowledgments

The authors wish to thank G. J. Lapeyre and U. Happek for many valuable discussions. Funding for this research was provided in part by the Air Force Office of Scientific Research under Grant No. F49620-00-1-0314. This material is based upon work partially supported under a National Science Foundation Graduate Research Fellowship. This work is based on research conducted in part at the Synchrotron Radiation Center, University of Wisconsin-Madison, which is supported by the National Science Foundation under award No. DMR-0084402.

References

- [1] See, for example, Hufner, S., 1978, *Optical Spectra of Transparent Rare Earth Compounds*, (New York: Academic Press).
- [2] Hamilton, D. S., Gayen, S. K., Pogatshnik, G. J., Ghen, R. D., and Miniscalco, W. J., 1989, *Phys. Rev. B*, **39**, 8807.
- [3] Lawson, J. K., and Payne, S. A., 1993, *Phys. Rev. B*, **47**, 14003.
- [4] Mayolet, A., Zhang, W., Simoni, E., Krupa, J. C., and Martin, P., 1995, *Optical Materials*, **4**, 757.
- [5] Pedrini, C., McClure, D. S., and Anderson, C. H., 1979, *J. Chem. Phys.*, **70**, 4959.
- [6] Pedrini, C., Rogemond, F., and McClure, D. S., 1986, *J. Appl. Phys.*, **59**, 1196.
- [7] Raukas, M., Basun, S. A., van Schaik, W., Yen, W. M., and Happek, U., 1996, *Appl. Phys. Lett.*, **69**, 3300.
- [8] Wertheim, G. K., Rosencwaig, A., Cohen, R. L., and Guggenheim, H. J., 1971, *Phys. Rev. Lett.*, **27**, 505.
- [9] Dujardin, C., Pedrini, C., Gâcon, J. C., Petrosyan, A. G., Belsky, A. N., and Vasil'ev, A. N., 1997, *J. Phys.: Condens. Matter*, **9**, 5229.
- [10] Thiel, C. W., Cruguel, H., Wu, H., Sun, Y., Lapeyre, G. J., Cone, R. L., Equall, R. W., and Macfarlane, R. M., 2001, *Phys. Rev. B*, **64**, 085107.
- [11] Blasse, G., Schipper, W., and Hamelink, J. J., 1991, *Inorg. Chim. Acta*, **189**, 77.
- [12] Thiel, C. W., Cruguel, H., Sun, Y., Lapeyre, G. J., Macfarlane, R. M., Equall, R. W., and Cone, R. L., 2001, *J. Lumin.*, **94-95**, 1.
- [13] Thiel, C. W., Cruguel, H., Wu, H., Sun, Y., Lapeyre, G. J., Cone, R. L., Equall, R. W., and Macfarlane, R. M., 2001, *Opt. & Phot. News*, **12** (12), 64.
- [14] van Pieterse, L., Heeroma, M., de Heer, E., Meijerink, A., 2000, *J. Lumin.*, **91**, 177.
- [15] Moine, B., Courtois, B., and Pedrini, C., 1989, *J. Phys. France*, **50**, 2105.
- [16] Sellin, P. B., Strickland, N. M., Carlsten, J. L., and Cone, R. L., 1999, *Opt. Lett.*, **24**, 1038.
- [17] Sellin, P. B., Strickland, N. M., Böttger, T., Carlsten, J. L., and Cone, R. L., 2001, *Phys. Rev. B*, **63**, 155111.
- [18] Babbitt, W. R. and Mossberg, T. W., 1986, *Appl. Opt.*, **25**, 962.
- [19] Saari, P., Kaarli, R., and Rebane, A., 1986, *J. Opt. Soc. Am. B*, **3**, 527.
- [20] Macfarlane, R. M. and Shelby, R. M., 1987, in *Spectroscopy of Solids Containing Rare Earth Ions*, edited by Kaplyanski, A. A. and Macfarlane, R. M. (Amsterdam: North Holland), pp. 51—184.
- [21] Macfarlane, R. M. and Wittmann, G., 1996, *Opt. Lett.*, **21**, 1289.
- [22] Ohlsson, N., Mohan, R. K., and Kröll, S., 2002, *Opt. Commun.*, **201**, 71.
- [23] Sellars, M. J., (private communication).
- [24] Sun, Y., Thiel, C. W., Cone, R. L., Equall, R. W., and Hutcheson, R. L., 2002, *J. Lumin.*, accepted for publication.
- [25] Fadley, C. S., Hagström, S. B. M., Klein, M. P., and Shirley, D. A., 1968, *J. Chem. Phys.*, **48**, 3779.
- [26] Citrin, P. H. and Thomas, T. D., 1972, *J. Chem. Phys.*, **57**, 4446.
- [27] Poole, R. T., Szajman, J., Leckey, R. C. G., Jenkin, J. G., and Liesegang, J., 1975, *Phys. Rev. B*, **12**, 5872.
- [28] Johansson, B., 1974, *J. Phys. F*, **4**, L169.

- [29] Johansson, B. and Mårtensson, N., 1980, *Phys. Rev. B*, **21**, 4427.
- [30] Lang, J. K., Baer, Y., and Cox, P. A., 1981, *J. Phys. F*, **11**, 121.
- [31] Thiel, C. W., Sun, Y., and Cone, R. L., (unpublished).
- [32] Martin, W. C., Zalubas, R., and Hagan, L., 1978, *Natl. Stand. Ref. Data Ser.* (U.S.: Natl. Bur. Stand.), Vol. 60.
- [33] Weber, M. J., 1973, *Solid State Commun.*, **12**, 741.
- [34] Dorenbos, P., 2000, *J. Lumin.*, **91**, 91.
- [35] Jørgenson, C. K., 1962, *Mol. Phys.*, **5**, 271.
- [36] McClure, D. S., and Kiss, Z., 1963, *J. Chem. Phys.*, **39**, 3251.
- [37] Loh, E., 1966, *Phys. Rev.*, **147**, 332.
- [38] Brewer, L., 1971, *J. Opt. Soc. A.*, **61**, 1666.
- [39] Dorenbos, P., 2000, *J. Lumin.*, **91**, 155.

Tables

Table I. Effective free-ion ionization potentials for the trivalent rare earth ions determined from the systematic deviations between the experimental 4f electron binding energies in optical materials and the empirical model for the binding energies. The errors were determined from the experimental errors of the measurements that contributed to each estimate.

<i>Rare Earth Ion</i>	<i>Effective Ionization Potential (eV)</i>	<i>Estimated Error (eV)</i>
Ce ³⁺	36.757	±0.005
Pr ³⁺	38.98	±0.02
Nd ³⁺	40.52	±0.14
Pm ³⁺	41.0	±0.6
Sm ³⁺	41.51	±0.14
Eu ³⁺	42.94	±0.29
Gd ³⁺	44.40	±0.12
Tb ³⁺	39.37	±0.07
Dy ³⁺	41.35	±0.12
Ho ³⁺	42.47	±0.12
Er ³⁺	42.56	±0.12
Tm ³⁺	42.52	±0.12
Yb ³⁺	43.53	±0.09
Lu ³⁺	45.25	±0.03

Figure Captions

Figure 1. Energy level diagram illustrating the photon-gated photoionization spectral hole burning process in rare-earth-activated materials.

Figure 2. Comparison of empirical 4f electron binding energy models. Circles represent measured 4f electron binding energies relative to the Fermi energy in the elemental rare-earth metals from Ref. [30]. The dotted line is the fit of the empirical model using the ions' atomic numbers. The solid line is the fit of the empirical model using the ions' radii.

Figure 3. Comparison of the empirical model using the free-ion ionization potentials and using the effective ionization potential values from Table 1. Circles represent average experimental 4f electron binding energies relative to the valence band maximum in yttrium aluminum garnet from Refs. [2, 6, 10]. The dotted line is the fit of the binding energy model using the free-ion ionization potentials. The solid line is the fit of the binding energy model using our empirical values for the ionization potentials given in Table 1.

Figure 4. The $4f^N$ and $4f^{N-1}5d$ binding energies in rare-earth-activated yttrium aluminum garnet (YAG) relative to the host valence band. Circles represent average measured $4f^N$ binding energies from Refs. [2, 6, 10] and the solid line is the fit of the $4f^N$ binding energy model using the effective ionization potentials from Table 1. Triangles represent $4f^{N-1}5d$ binding energies determined from the $4f^N$ binding energy model and measured $4f^N$ to $4f^{N-1}5d$ transition energies from Refs. [33, 34]. The dotted lines represent the model for the $4f^{N-1}5d$ binding energies; the upper line corresponds to the lowest energy high-spin state and the lower line corresponds to the lowest energy low-spin state.

Figures

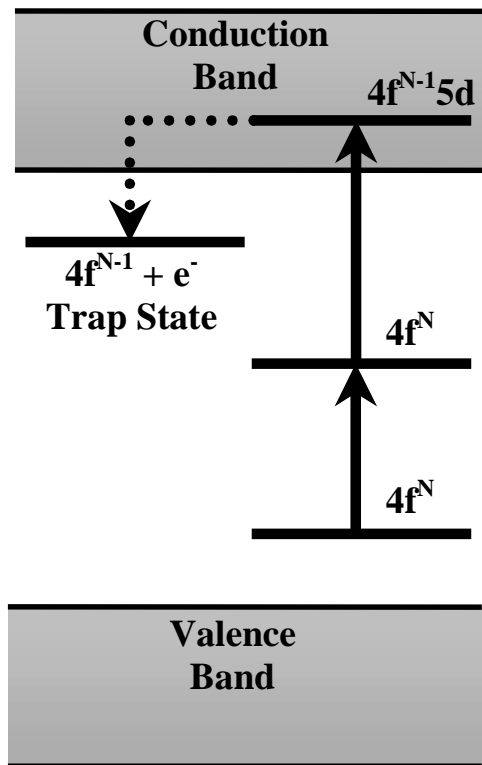


Figure 1. Energy level diagram illustrating the photon-gated photoionization spectral hole burning process in rare-earth-activated materials.

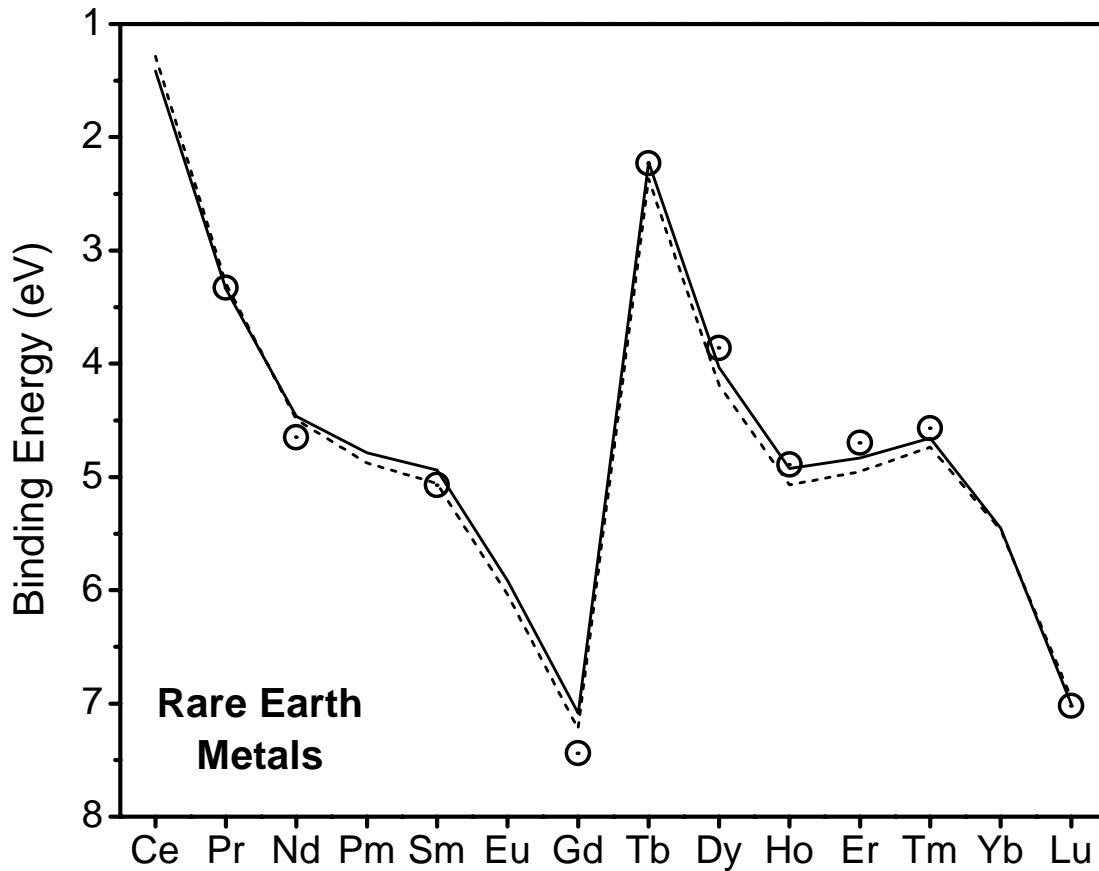


Figure 2. Comparison of empirical 4f electron binding energy models. Circles represent measured 4f electron binding energies in the elemental rare-earth metals from Ref. [30]. The dotted line is the fit of the empirical model using the ions' atomic numbers. The solid line is the fit of the empirical model using the ions' radii.

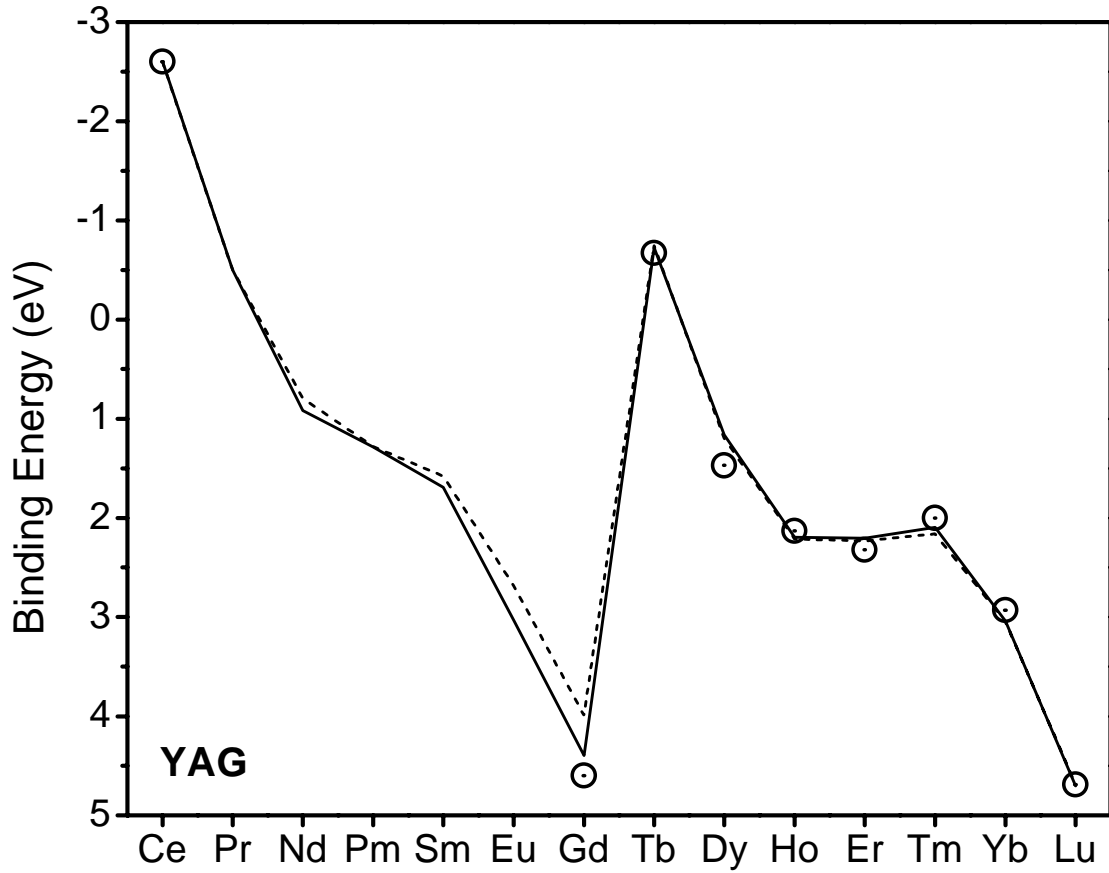


Figure 3. Comparison of the empirical model using the free-ion ionization potentials and using the effective ionization potential values from Table 1. Circles represent average experimental 4f electron binding energies in yttrium aluminum garnet from Refs. [2, 6, 10]. The dotted line is the fit of the binding energy model using the free-ion ionization potentials. The solid line is the fit of the binding energy model using our empirical values for the ionization potentials given in Table 1.

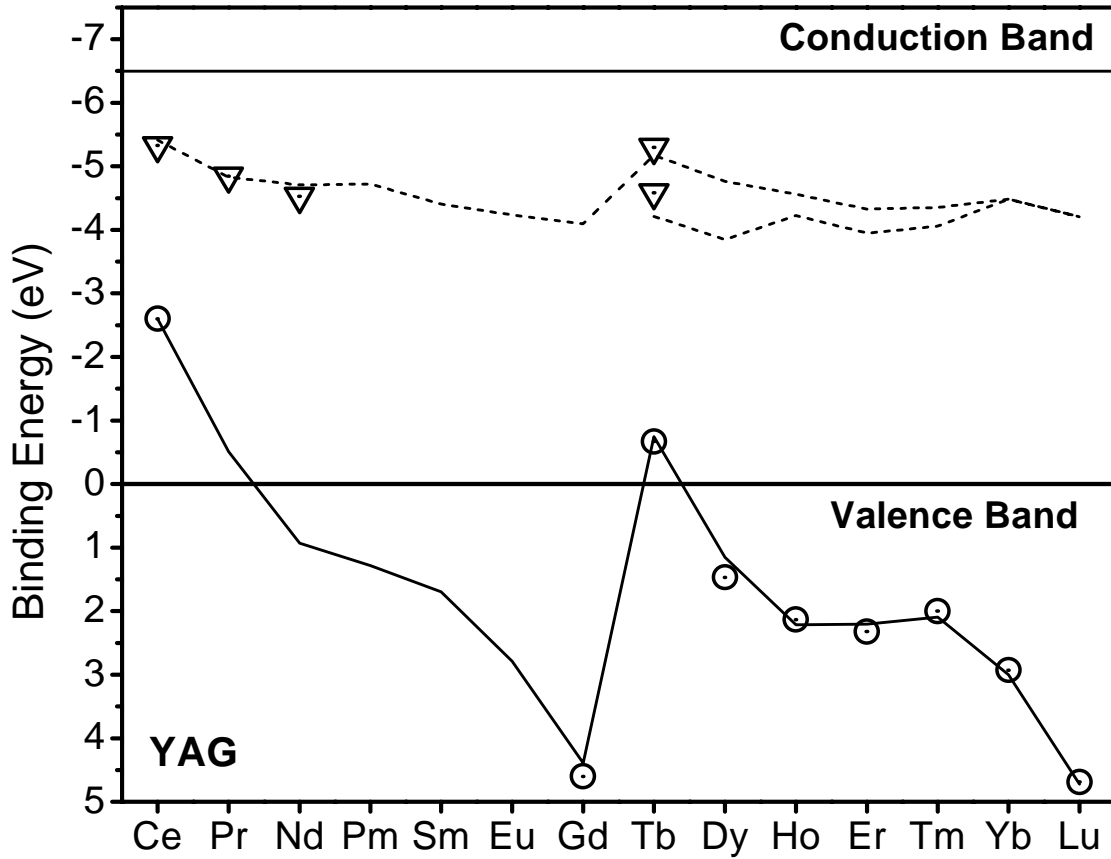


Figure 4. The $4f^N$ and $4f^{N-1}5d$ binding energies in rare-earth-activated yttrium aluminum garnet (YAG) relative to the host valence band. Circles represent average measured $4f^N$ binding energies from Refs. [2, 6, 10] and the solid line is the fit of the $4f^N$ binding energy model using the effective ionization potentials from Table 1. Triangles represent $4f^{N-1}5d$ binding energies determined from the $4f^N$ binding energy model and measured $4f^N$ to $4f^{N-1}5d$ transition energies from Refs. [33, 34]. The dotted lines represent the model for the $4f^{N-1}5d$ binding energies; the upper line corresponds to the lowest energy high-spin state and the lower line corresponds to the lowest energy low-spin state.